Global Advanced Research Journal of Medicine and Medical Science (ISSN: 2315-5159) Vol. 4(9) pp. 366-382, September, 2015
Available online http://garj.org/garjmms

Full Length Research Paper

Screening of *Fusarium* spp Resistance to Silver Ions for Ability to Synthesize Silver Nanoparticles from Egyptian Soils

Mohamed Medhat Ghareib[1], Magdy Attia[2], Nemat M. Awad[2], Magdi Z. Matter[1] and Dina El-Kahky[1]*

[1]Botany Department, Faculty of Science, Menoufia University, Cairo, Egypt.
[2]Agricultural Microbiology Department, National Research Centre, 33 El-Bohouth Street, (former El- Tahrir Street,) Dokki, Giza, Egypt. Postal Code: 12622.

Accepted 31 August, 2015

Six isolates of *Fusarium* (T18, T22, TA, MB, KHG and KHD) were resistant to up to 2 mM silver nitrate. These isolates were screened for their ability to synthesize silver nanoparticles from silver nitrate ($AgNO_3$). From the results of colour change and UV-Visible spectra, only three isolates (T18, TA, and KHG) showed brown colour and strong surface plasmon resonance centered at around ca. 420 nm, is characteristic of colloidal silver. Hence, further work was carried out with these isolates. These *Fusarium* strains that were to synthesize silver nanoparticles were identified as the general *Fusarium oxysporum, Fusarium graminearum* and *Fusarium solani,* based on the morphological characteristics and sequence analysis of 18S rRNA. The extracellular productions of silver nanoparticles by the three strains of *Fusarium* were investigated. It was found that exposure of *Fusarium* to silver ion leads to the formation of silver nanoparticles. The nanoparticles were examined using UV-Visible spectroscopy, Transmission Electron Microscopy (TEM), X-ray Diffraction (XRD), and Fourier Transform Infrared Spectroscopy (FTIR) analysis. The silver nanoparticles were in the range of 5-80 nm in dimension.

Keywords: Egyptian soils, *Fusarium* spp., silver ion, silver nanoparticles ,FTIR, TEM, UV, XRD.

List of Abbreviations

FTIR, Fourier Transform Infrared Spectroscopy Analysis; KH, Kafr El-Sheikh; M, El-Mahalla; NPs, nanoparticles; SEM, scanningelectron microscope; T, Tanta; TEM, transmission electron microscope; X-ray spectroscopy

INTRODUCTION

The term nanoparticle is used to describe a particle with size in the range of 1-100 nm (Yehia and Al-Sheikh, 2014). They tend to react differently than larger particles of the same composition because of their large surface area, thus allowing them to be used in novel applications (Abou El-N et al., 2010). Moreover, they serve as the fundamental building block of nanotechnology (Vahabi et al., 2011) Nowadays there is a wide application of nanoparticles in diverse fields including catalysis, energy,

*Corresponding Author E-mail: d_elkahkey@yahoo.com; Tel.: +20123268805, 0202 22620373; Fax: 0202 6203731

chemistry and medicine (Yehia and Al-Sheikh, 2014). Nanotechnology approaches to control disease in human and plants have recently been increasing greatly and the unique physicochemical properties of nano-sized metal particles make them successful in biology and medicine (Jo et al., 2012).

The current understanding of potential risks associated with the release of these materials in the environment for human and

animal health is still insufficient (Wang et al., 2012). However, very recently (Verano-Braga et al., 2014) reported that the toxicity of AgNPs depends upon both dosage and particle size. Metal nanoparticles show large surface to volume ratio and exhibit antimicrobial properties due to their ability to interact with cellular membranes through disruption of cell wall structure (Ahmad et al., 2013; Trop et al., 2006). Especially silver has long been known for its strong toxicity against a wide range of microorganisms including bacteria and fungi (Narayanan and Park, 2014). There are numerous methods for synthesis of silver nanoparticles, but, mostly used chemical methods, including toxic chemicals and mostly non-polar solvent. Therefore, there is tremendous need for the development of clean and biocompatible as well as cost effective and sustainable method for synthesizing silver nanoparticles. According to (Bansal et al., 2011) biological methods of silver nanoparticles synthesis require a special ability: “Resistance of the organism to silver ions. The fungi are extremely good candidates in the synthesis of metal nanoparticles. The use of fungi for the production of nanoparticles is under explored in the literature. Fungi have only been used to produce only a few types of nanoparticles, and research in this area has only gained attention in the last few years. The main advantages of using fungi over bacteria for NPs synthesis are: 1) Their large biomass enables easy handling during biosynthesis (Binupriya et al., 2010). 2) High metal tolerance (Narayanan and Sakthivel, 2011). 3) Bioaccumulation ability (Gupta and Devi). 4) Larger protein secretions (Du et al., 2011). 5) Ease of scale up (Narayanan and Sakthivel, 2011). 6) Economic viability (Narayanan and Sakthivel, 2011). 7) High wall binding ability (Sheikhloo et al., 2011).

The fungi are extremely good candidates in the synthesis of metal nanoparticles. Due to the development and attractiveness of nanotechnology, the production and use of engineered nanoparticles (NPs, defined by a size below 100 nm) strongly increased during the last decades, in particular in USA, Europe and East Asia Woodrow Wilson International Centre for Scholars, (Nel et al., 2006; Wiesner et al., 2006). This rapid proliferation can be explained by the special physical and chemical properties of these structures, due to their high surface area and reactivity in comparison to the bulk material (Auffan et al., 2009).

(Rai et al., 2009) proposed the term “Myconanotechnology” for the synthesis of nanoparticles by using fungi. Application of fungi for production of SNPs is potentially exciting because of their ability to secrete large amount of proteins (Vahabi et al., 2011) Among various metals, silver has been in use since antiquity in the form of metallic silver, silver nitrate, and silver sulfadiazine. But due to the arrival of several antibiotics, the use of these silver compounds has been weakened remarkably. Use of silver has been again realized in the form of SNPs, which show the significant antimicrobial activity against the multidrug resistant microorganisms owing to their reduced size. Due to antimicrobial activity, SNPs are extensively used in dental materials (Chladek et al., 2011), coating stainless steel in medical devices (Knetsch and Koole, 2011), cosmetics (Kokura et al., 2010) and water treatment (Sheng and Liu, 2011). Antibacterial activity of SNPs was studied by various groups (Birla et al., 2009; Lara et al., 2011), Due to vast emerging applications of SNPs in distinct fields, there is increase in demand for SNPs, and to fulfil the demand, there is a pressing need to increase their yield, for which optimization of the process is very important step. A little contribution has been made regarding the effect of cultural and physical conditions on the biosynthesis of SNPs. The synthesis of SNPs at nano range is still a challenge. In order to increase the yield and the shelf-life (stability) of SNPs with minimum investment, it is necessary to optimize the cultural conditions and various physical parameters like pH, light intensity, and temperature. To our knowledge, there is no prior report on the optimization of all these conditions for large scale synthesis of SNPs.

The purpose of the present study was involves biosynthesis, characteristic and manipulate the conditions favours the production of silver nanoparticles by some isolates of *Fusarium* spp. isolated from different Egyptian soils Environment and resistance to silver ions

MATERIALS AND METHODS

Screening of *Fusarium* isolates ability to synthesis silver nanoparticles

To prepare biomass for biosynthesis studies, the fungi were grown aerobically in a liquid media containing Glucose, 31.57g; $NaNo_3$, 2.0g; KH_2P0_4, 1.0g; $MgS0_4$.7H2O, 0.5g; KC1, 0.5g; $FeCl_3$.6H2O, 0.001g; Distilled water,1000 ml and pH 7.10-7.50, media in 250 ml Erlenmeyer flasks. The flasks were inoculated and incubated on an orbital shaker at 28±2 °C and agitated at 150 rpm. The biomass was harvested by sieving through a plastic sieve, followed by extensive washing with Milli-Q deionized water to remove any medium component from the biomass. Typically 20 g of fresh biomass was brought in contact with 100 ml of Milli-Q deionized water for 72 hrs at 28±2 °C in an Erlenmeyer flask and agitated in the same condition as described earlier. After incubation, the

cell filtrate was obtained by passing it through Whatmann filter paper No. 1.

Extracellular production of Silver nanoparticles (AgNPs)

Production of nanoparticles was done according to the method of (Ahmad et al., 2003). For synthesis of silver nanoparticles, silver nitrate (1mM) was mixed with 50 ml of cell filtrate in a 250 ml Erlenmeyer flask and agitated at for 5 minutes. Control treatment (without the silver ions) was also run along with the experimental flask. The selected isolates showed change colour from yellow to reddish brown and strong surface plasmon resonance centered at around ca.420 nm

Identification of the fungal isolate

Identification of the selected fungal isolate was carried out by morphological and microscopic observations followed by 18S rRNA gene sequencing.

Morphological characterization

Morphological characteristics of pure strains obtained from the screening experiments were studied using the procedures described by (Nelson et al., 1983; Leslie and Summerell, 2006). Morphological features such as the size and shape of the macroconidia were examined using light microscopy. Colony colour and colony diameter were recorded after 3, 7, and 10 days of growth on Potato Dextrose Agar.

DNA isolation, PCR amplification, and sequencing Genomic DNA was extracted using genomic DNA miniprep purification spin kit (Qiagen, Hilden, Germany). The universal 18S rRNA gene primers: forward nu-SSU-0817-5, 5'-TTAGCATGGAATAATRRAATA-3' and reverse nu-SSU-1536-3, 5'-ATTGCAATGCYCTATCCCCA-3' were used for amplification of the 18S rRNA gene. Amplification of DNA was carried out with a 9700 Gold thermal cycler (Applied Biosystems, Warrington, UK) under the following conditions: initial denaturation at 94 °C for 2 min; 35 cycles of denaturation at 94 °C for 0 min, annealing at 56□ for 10 sec, extension at 72 °C for 30 sec., and a final extension at 72 °C for 2 min. The amplified PCR product was analyzed on an agarose gel and the amplified DNA was purified using QIA quick gel extraction kit (Qiagen) which was subsequently sequenced using Big Dye terminator (Applied Biosystems). The resulting sequence was analyzed using the BLAST algorithm of National Centre of Biological Information (NCBI) database to obtain closely related phylogenetic sequences. The phylogenetic tree was constructed using Neighbour Joining method in MEGA ver. 4.0 software graph.

Optimization of physio-chemical parameters for biosynthesis of nanoparticles

Influence of substrate concentration (0.1, 0.5, 1, 1.5, 2.0 mM $AgNO_3$), pH, salinity and temperature on the production of silver nanoparticle was optimized by varying the parameters one at a time, such as pH (4, 5, 6, 7, 8), salinity (0.1, 0.2, 0.3, 0.4, 0.5%NaCl), temperature (15, 25, 35, 45 °C) and incubation period (0–120 h). Sample of 1ml was withdrawn at different time intervals and the absorbance was measured at 420 nm.

Characterization of silver nanoparticles

Ultraviolet-Visible (UV-Vis) Spectra Analysis

The bioreduction of the silver ions in the solution was monitored by sampling the aqueous component (1 ml) and measuring the UV-Vis spectrum of the solution. The optical characteristics were studied by scanning the sample from 200–800 nm. Sample of 1 ml was withdrawn at different time intervals and the absorbance was measured at a resolution of 1 nm using a UV–Vis spectrophotometer (UV-2401 PC).

Transmission Electron Microscope (TEM)

The cell filtrates of different isolates were used to form a film of silver nanoparticles on carbon coated copper TEM grids and analyzed under transmission electron microscopy (TECNAI 120) at a voltage of 120 kV (Williams, 1996).

X-Ray Diffraction Analysis (XRD)

The liquid reaction mixture after bioreduction was dried at 45 ºC in a vacuum drying oven. Then the dried mixture was collected for the determination of the formation of silver nanoparticles. The vacuum-dried silver nanoparticles were used for powder X-ray diffraction (XRD) analysis. The spectra were recorded according to WIN-FIT program (Krumm, 1995).

Protein purification

For the purification of proteins from aqueous cell-free filtrate, solid ammonium sulphate was added slowly to control solutions containing extracellular proteins at a final concentration of 80 % (w/v). Precipitate fraction was subsequently dialyzed using a 12-kDa cut-off membrane. The mixture was gently stirred for overnight at 4 ºC. The resulting precipitate was subsequently collected by centrifugation at 12000 rpm for 10 min at 4 ºC.

Electrophoresis of native protein (PAGE)

Protein extract supernatant was mixed with an equal volume of a solution containing 20 % glycerol (v/v) and 0.1 ml bromophenol blue in 0.15 M Tris-HCl, pH 6.8. Twenty microlitres of the resulting suspension (40 to 60 ug of protein) were subjected to electrophoresis in 25 mM Tris buffer containing 192 mM glycine at pH 8.3. Electrophoresis was conducted at 10 °C for 4 hrs. in a 7.5 % polyacrylamide gel with a 3.5 % stacking gel, at 15 and 30 mA, respectively, until the dye band reached the bottom of the separating gel (Laemmli, 1970). Electrophoresis was performed in a vertical slab mould (16x18x0.15 cm). Gels were stained with silver nitrate for the detection of protein bands (Sammons et al., 1981).

Fourier Transform Infrared Spectroscopy Analysis (FTIR)

For FTIR spectroscopy analysis, the vacuum dried silver nanoparticles were mixed with Potassium Bromide (KBr) at a ratio of 1:100 and the spectra were recorded with a SHIMADZU 8400S Fourier Transform Infrared Spectrophotometer using a diffuse reflectance accessory. The scanning data were obtained from the average of 49 scans in the range between 4000 to 400 cm^{-1}.

RESULTS AND DISCUSSION

Screening of *Fusarium* isolates ability to synthesis silver nanoparticles

Biological methods of silver nanoparticles synthesis require a special ability “Resistance of the organism to silver ions”. In this study, six isolates of *Fusarium* (T18, T22, TA, MB, KHG and KHD) were resistances to silver nitrate (up to 2 mM). These isolates were screening for their ability to synthesis silver nanoparticles from silver nitrate ($AgNO_3$). The fungal biomass was separated by filtration after the incubation period of 72 hrs. The pale yellow colour of the fungal cells filtrate can clearly after immersion in 1 mM silver nitrate ($AgNO_3$) solution for 24 hrs. It can be observed that the previous pale yellow colour of the reaction mixture is changed to the brownish colour after 24 hrs of reaction in case of T18, TA and KHG. The appearance of a yellowish-brown colour in solution containing the biomass was suggested as indicator of the formation of silver nanoparticles in the reaction mixture. The appearance of reddish brown colour solution clearly indicates the formation of silver nanoparticles (Sastry et al., 2002). While, in case of isolates T22, MB, KHD and negative control (silver nitrate solution alone), no change in colour was observed even after 72hrs and 10 days. Only three isolates (T18, TA and KHG) showed reddish brown colour. The UV-Vis spectra recorded after 72 hrs of reaction of *Fusarium* isolates with silver nitrate. The strong surface plasmon resonance centered at around ca.420 nm was observed for silver nanoparticles after 72 hrs of incubation and the intensity of the peak was found increasing as the progress of the reaction continues which explains an increase in the number of particles. The colour change was caused by the surface plasmon resonance (SPR) of silver nanocrystals in the visible region (Varshney et al., 2009). Silver nanocrystals are known to exhibit size and shape-dependent SPR bands which are characterized by UV–Visible absorption spectroscopy (Xie et al., 2007). This event clearly indicates that the reduction of the ions occur extracellularly through reducing agents released into the solution by fungi. No change in intensity at around ca.420 nm was observed indicating complete reduction of silver ions. An absorption band at around ca.270 nm was observed which indicated the presence of tryptophan and tyrosine residues in proteins. The strong surface plasmon resonance centered at around ca.420 nm was observed for silver nanoparticles after 72 hrs of incubation. The result obtained is similar to the observations made by (Durán et al., 2005) where *F. oxysporum* 07SD strain has been used for synthesizing silver nanoparticles by intra- and extracellular methods. From the results of colour change and UV-Visible, only three isolates (T18, TA, and KHG) showed brown colour and strong surface plasmon resonance centered at around ca. 420 nm, is characteristic of colloidal silver. Hence, further work was carried out with only these isolates. Hence, further work was carried out with only these isolates.

Identification of selected *Fusarium* isolates

The three fungal isolates (T18, TA and KHG) were purified by single spore culture method and identified with the help of relevant literature (Elfatih et al., 2002; Haware et al., 1992; Saxena et al., 1987; Murumkor and Chavan, 1985). Morphologically the colony of *Fusarium* spp. on PDA varies widely. Mycelia may be floccose, sparse or abundant and range in colour from white to pale violet. *F. oxysporum* usually produces a pale to dark-violet or dark-magenta pigments in the agar but some isolates produce no pigment at all. The critical morphological features of *Fusarium* spp. include the production of microconidia in false heads on short phialides formed on the hyphae, the production of chlamydospores arid the shape of the macroconidia and the microconidia (Seifert, 1996). Cultures of *F. solani* usually are white to pink with sparse mycelium. Sporodochia often are produced in abundance and may be cream, blue or green. Many isolates do not produce pigments in the agar although some violet or brown pigments may be observed (Ingle et al., 2009). Based on the morphological characteristics and sequence analysis of 18S rRNA, (Figure 1) *Fusarium* strains (TA, KHG and T18) capable of synthesize silver nanoparticles belong to the general *F. oxysporum, F. graminearum* and *F. solani*, respectively.

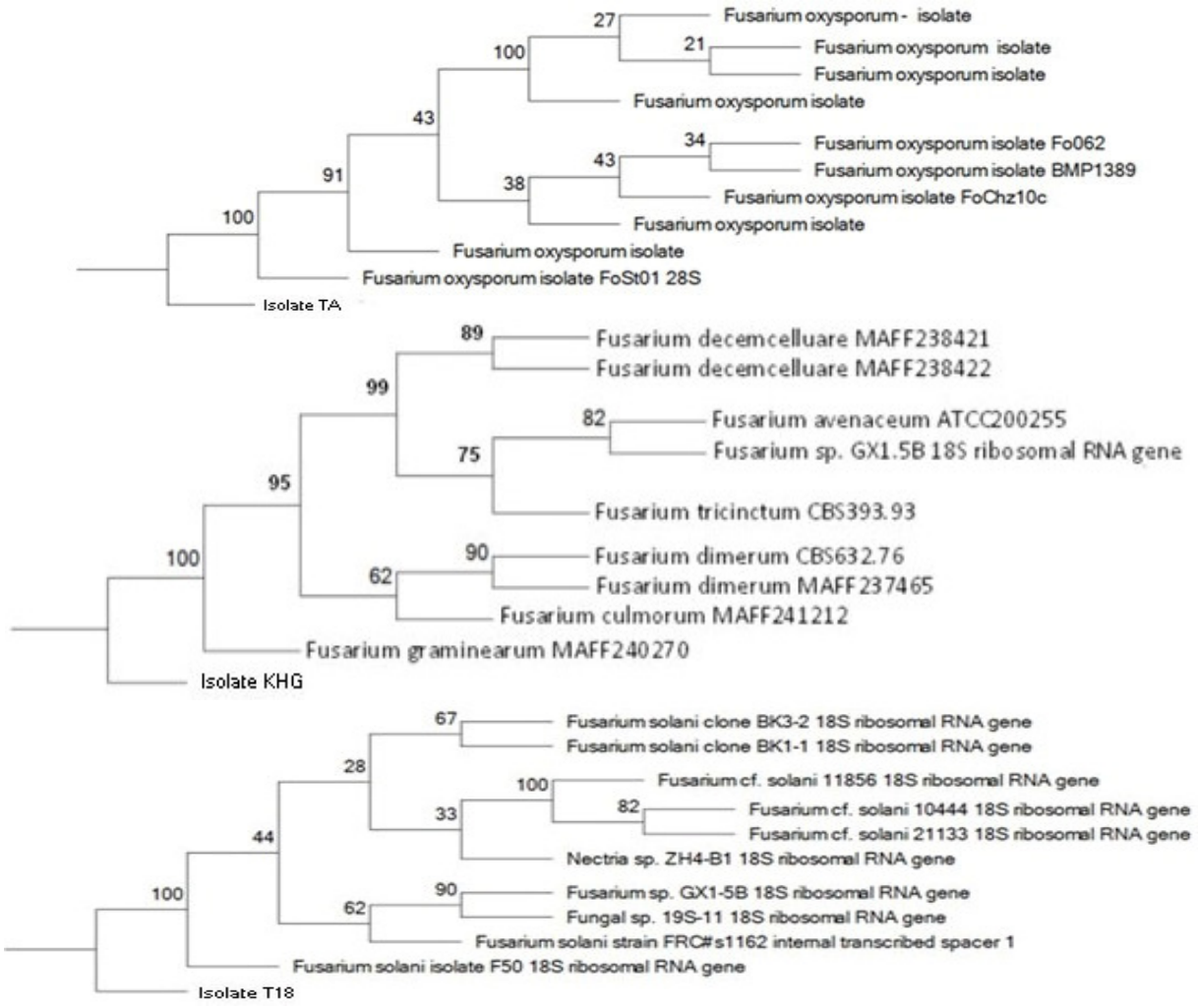

Figure 1. Phylogenetic tree of fungal isolate *F. oxysporum* (TA), *F. graminearum* (KHG) and *F. solani* (T18) and relationship among the selected strains based on sequencing analysis and the most closely related fungus species

Optimization of biosynthesis silver nanoparticles

Sathishkumar (Sathishkumar et al., 2009) studied the effects of biomaterial dosage, pH and temperature on nanoparticles formation. These factors have a major effect on the size and shape of the nanoparticles (He et al., 2002; Balaji et al., 2009).

The effect of substrate concentration

The effect of substrate concentration was studied by utilizing different concentrations of silver nitrate to synthesis the nanoparticles. Cell filtrate was treated with 0.1, 0.5, 1.0, 1.5, 2.0, 2.5 mM of silver nitrate (AgNO3) and incubated. The maximum production was observed at 1.5 mM concentration as shown in (Figure 2). The present study achieved the extracellular biosynthesis of silver nanoparticles within 72 hrs of incubation with silver ions. The F. oxysporum shows the beast isolated to produce AgNPs (Figure 1). The UV-Vis absorption intensity increased with increasing AgNO3 concentration, which reflects the formation of more silver nanoparticles. However, the absorption maximum was a little different when the AgNO3 concentration was varied from 1 to 1.5 mM/l. The maximum absorption peak existed at a lower wavelength when AgNO3 concentration was 1.5 mM/l. It is because the more AgNO3 molecules the more silver nuclei, then the more Ag nanoparticles with smaller sizes formed. The maximum absorption gave rise to a red shift from 404.2 to 418.4 nm when the AgNO3 concentration was increased from 0.033 to 0.050 mol/l, meaning the particle size increased (Chepuri and Trivedi, 2005; Courrol et al., 2007) and large silver aggregates formed. It is believed that the formation rate of nuclei increased significantly with increasing the AgNO3 concentration.

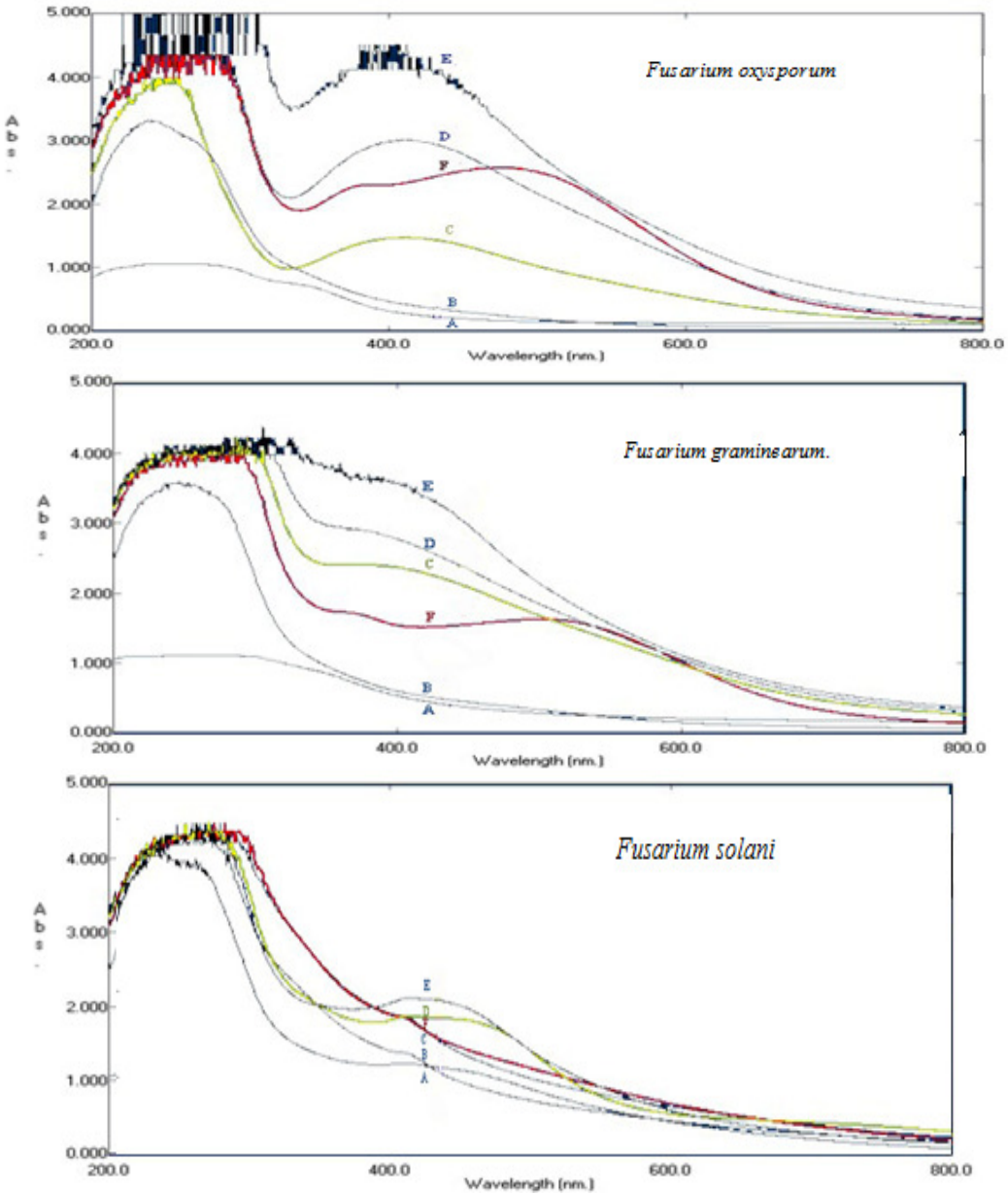

Figure 2. UV-Visible spectra recorded after 72 hrs of reaction of an aqueous solution of (0.1, 0.5, 1, 1.5 and 2.0 mM) silver nitrate with the fungal biomass *F. oxysporum, F. graminearum* and *F. solani*. A= control, B= 0.1 mM, C= 0.5 mM, D= 1 mM, E =1.5 mM, F= 2 mM. . Each value is mean ± standard error

The effect of pH

The effect of varying pH on the biosynthesis of silver nanoparticles by three *Fusarium* isolates is depicted in (Figure 3). It can be clearly seen from the UV-Visible absorption spectra that the absorption maxima shows the sharp peak at pH 6 compared to other values (pH 5, 7 and 8). This observation can be attributed to the capping proteins secreted. Similar study, pH 6 supported the maximum synthesis of silver nanoparticles (Kathiresan et al., 2009) whereas optimum gold accumulation by microbial cells normally occurs in the pH range of 2–6 (Joerger and Klaus, 2000) and changes in the pH has an effect on the size of gold nanoparticles (Mukerjee et al., 2001b). It was also proved that maximum production occurred at pH 6, as the highest absorbance was seen at this pH. At higher and lower pH, the absorbance was proportionately lower. It can be clearly seen from the UV-Visible absorption spectra that the absorption maximum shows the sharp peak at pH 6 but at pH 4 the broadening of absorbance is observed for AgNPs solution indicating the aggregation of particles.

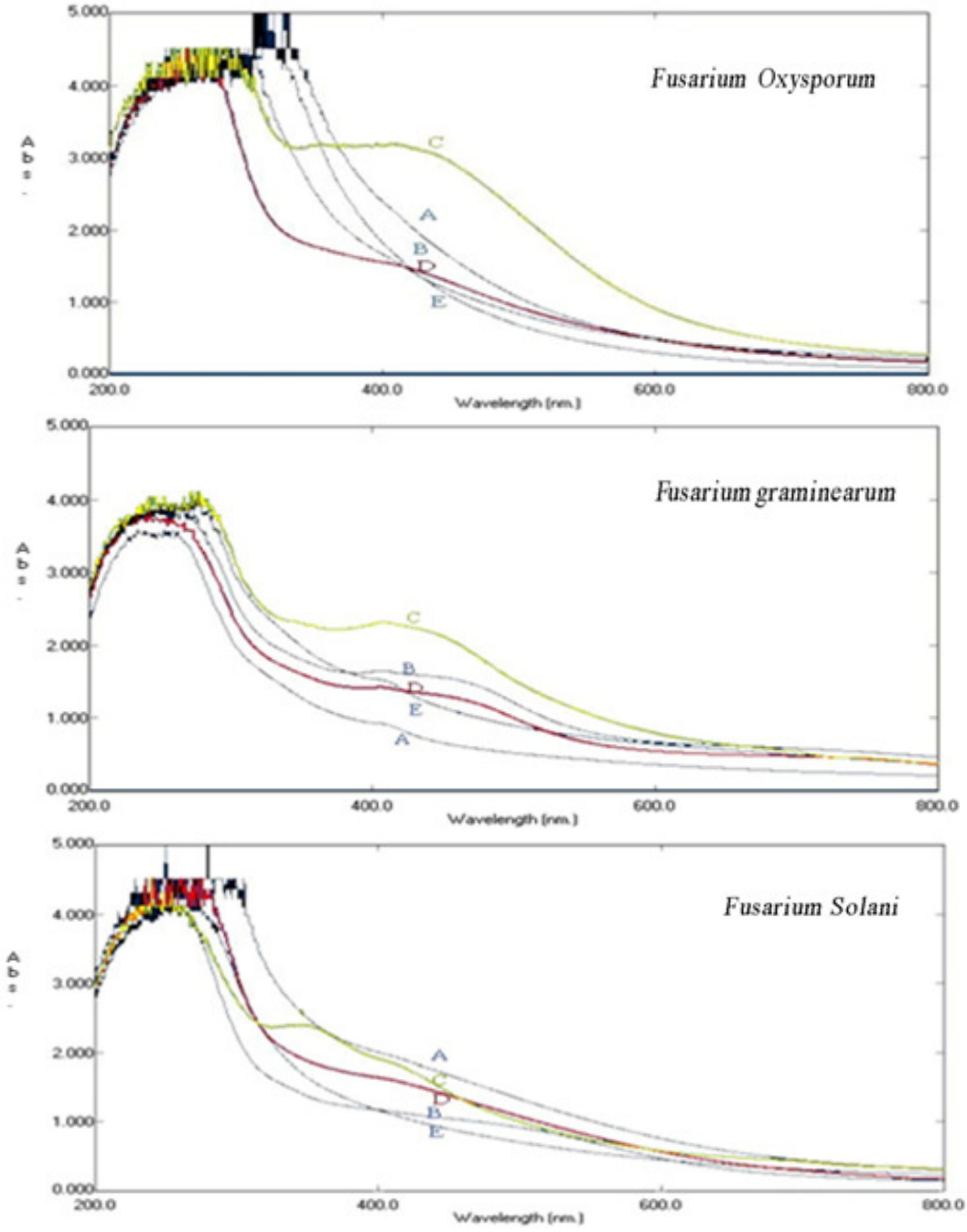

Figure 3. UV-Visible spectra recorded after 72 hrs of reaction of an aqueous solution of 1mM silver nitrate at different pH values with the fungal biomass *F. oxysporum, F. graminearum* and *F. solani*. A= pH 4, B= pH 5, C= pH 6, D= pH 7, E= pH 8. Each value is mean ± standard error

The effect of temperature

The effect of varying temperature on silver nanoparticle production by three isolates of *Fusarium* is presented in Figure 3. Study temperature range is from 15 to 45 °C and maximum production was attained from 25 to 35 °C. Temperature is an essential factor affecting silver nanoparticles production. Our present data indicates that the optimum temperature of 25 °C is rather specific for silver nanoparticles production by *Fusarium* (Figure 3) which shows maximum absorbance at O.D ca. 420 nm. *F. oxysporum* shows that the best isolated for synthesis AgNPs (Figure 4). Temperature is an essential factor affecting silver nanoparticles production (He et al., 2002; Balaji et al., 2009).

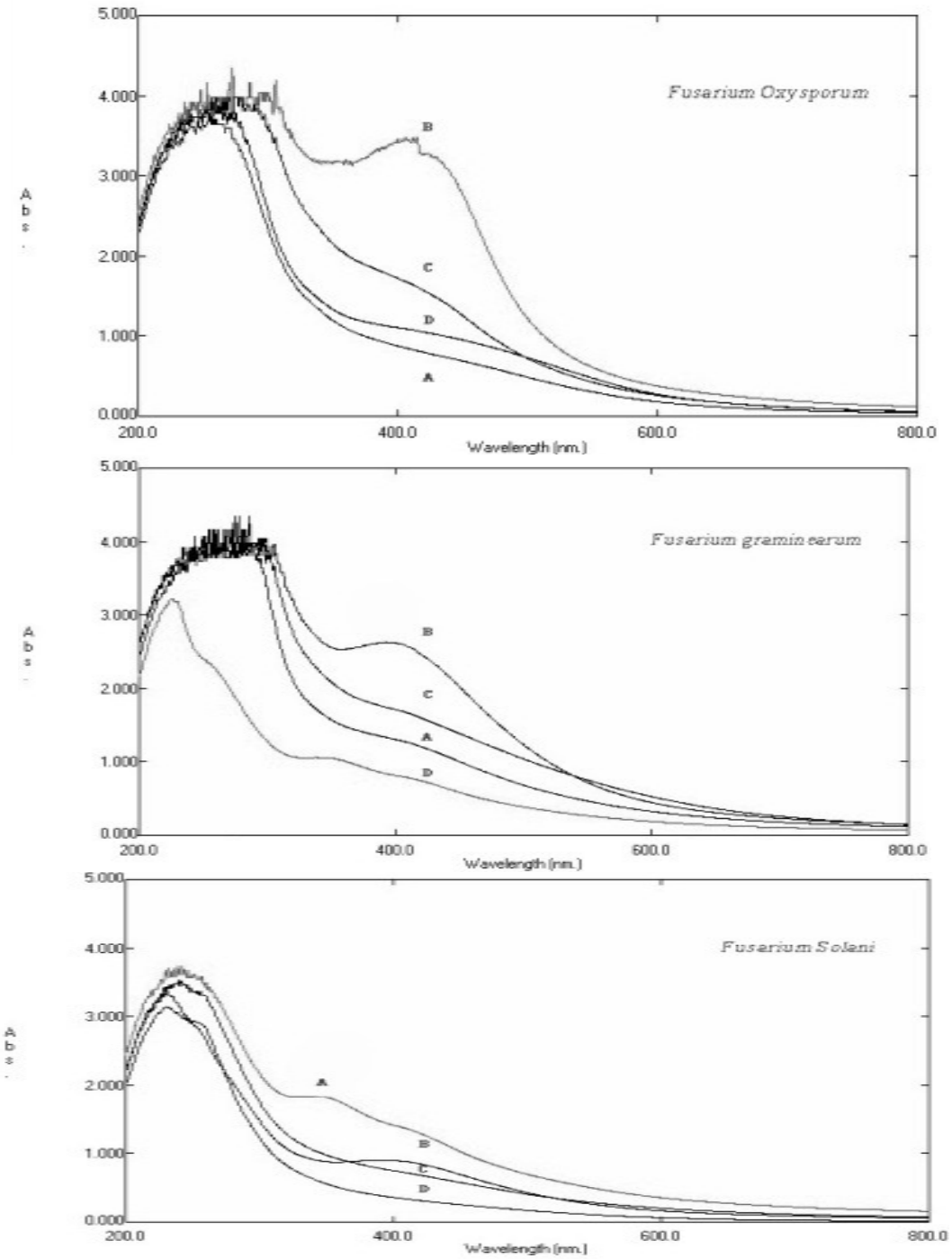

Figure 4. UV-visible spectra recorded after 72 hrs of reaction of an aqueous solution of 1mM silver nitrate at different temperature with the fungal biomass *F. oxysporum, F. graminearum* and *F. solani*. A= 15 °C, B= 25 °C, C= 35 °C, D= 45 °C. Each value is mean ± standard error and Comparison between isolates at O.D ca.420 nm

The effect of salinity

Silver nanoparticles synthesis was studied at different salinity values (0.1, 0.2, 0.3, 0.4 and 0.5 % NaCl) (Figure 5). Maximum production was observed at a salt concentration of 0.1%. It was also observed that concentrations of NaCl above 0.3 % were unfavorable for the nanoparticles synthesis. The concentrations of 0.1 %, 0.2 %, 0.3 % NaCl favored the production and stability of metal nanoparticles. *F. oxysporum* shows that the best isolated for synthesis AgNPs.

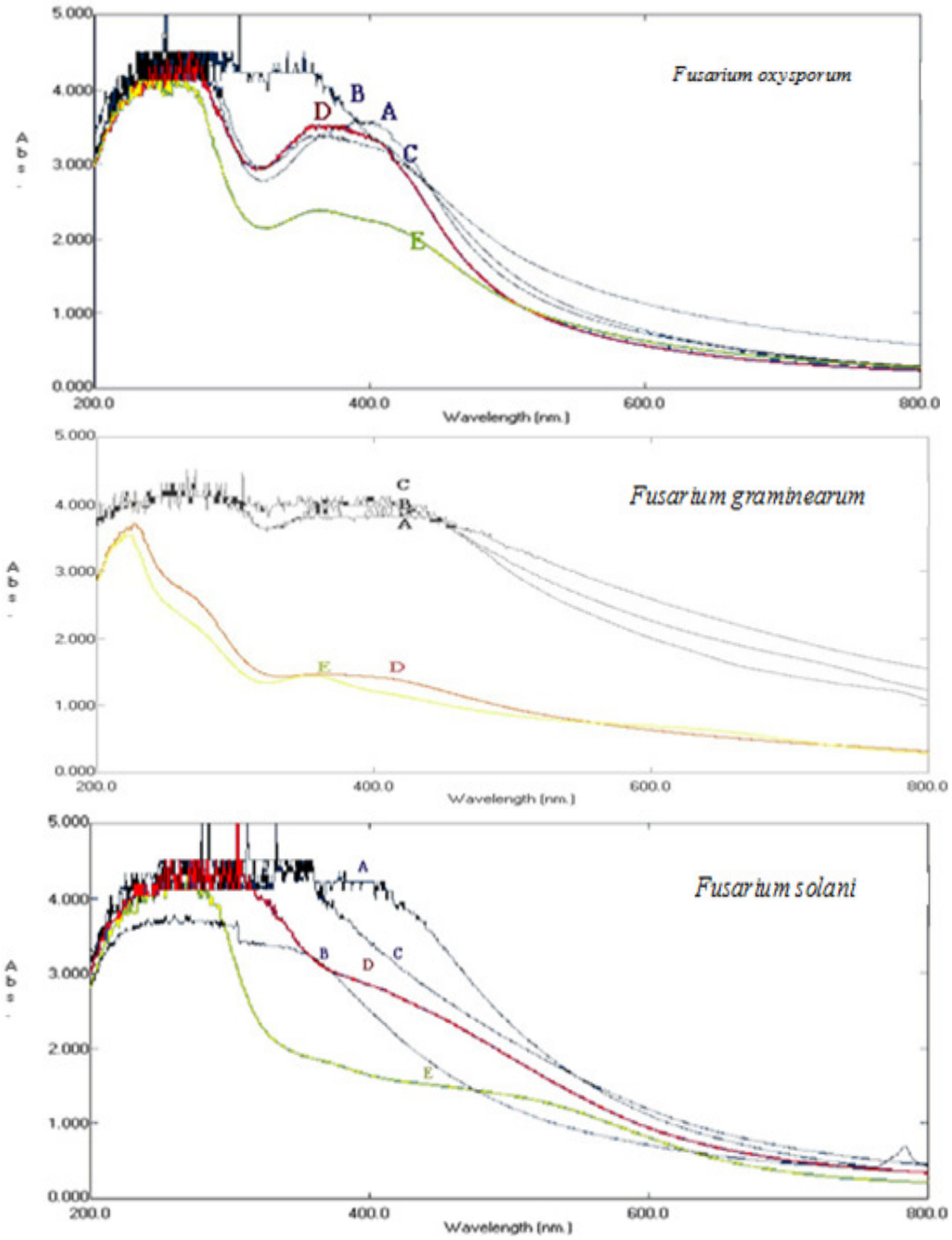

Figure 5. UV-Visible spectra recorded after 72 hrs of reaction of an aqueous solution of 1mM silver nitrate at different salinity values with the fungal biomass *F. oxysporum*, *F. graminearum* and *F. solani*. A= 0.1 % NaCl, B= 0.2 % NaCl, C= 0.3 % NaCl, D= 0.4 % NaCl, E= 0.5 % NaCl. Each value is mean±standard error

Effect of different incubation time on fungal growth on the synthetic silver nanoparticles

The presence of nanoparticles was confirmed using UV-Visible spectrophotometer for a complete wavelength scan of 200 to 800 nm. The absorbance measurements of the tested filtrate for 0 to 120 hrs are given in Figure 5. The time at which the aliquots were removed for measurement is indicated next to the respective curves. Results indicate that the absorbance values peak at around ca.420 nm at all time intervals with maximum values being observed after a period of 72 hrs (Petit et al., 1993; Li et al., 2007). The spectra clearly show the increase in intensity of silver solution with time reaction. In addition to the peak at 420 nm another peak at 378 nm is also seen that increases in intensity with time and

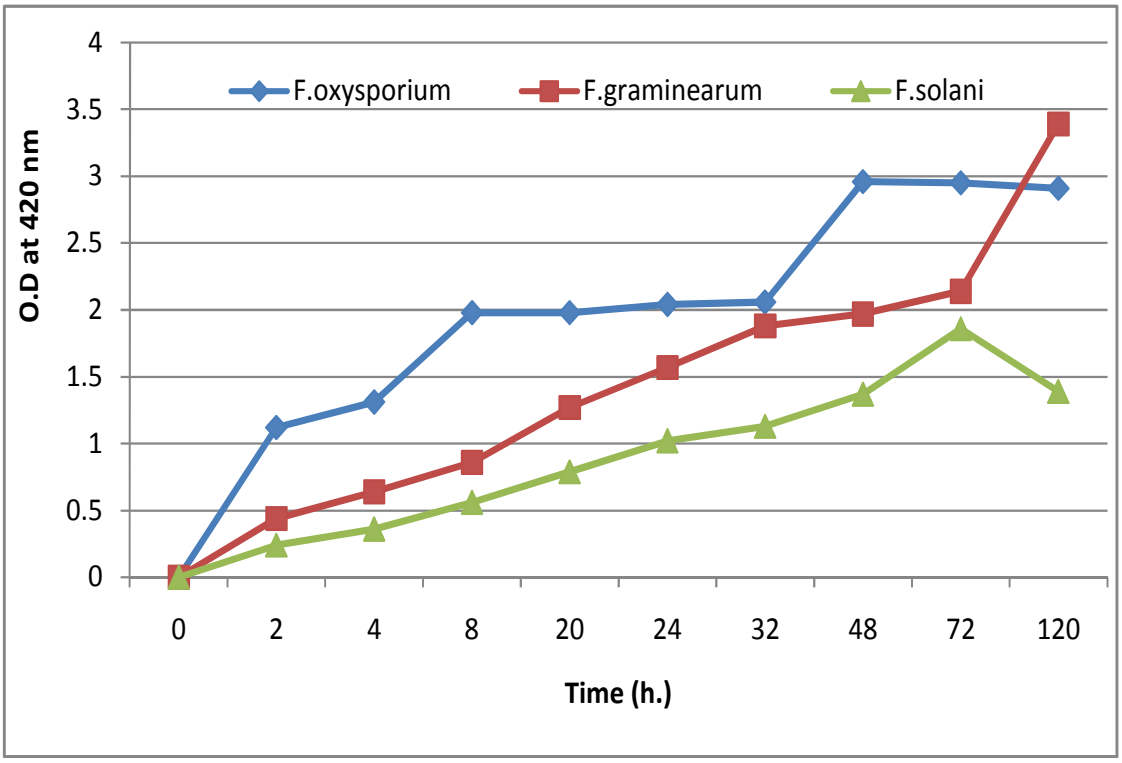

Figure 6. Comparison between isolates at O.D ca.420 nm of aqueous medium containing cell filtrate and silver ions (1 mM) in different time (0, 2, 4, 8, 20, 24, 32, 48, 72 and 120 hrs) Parametric optimization studies revealed that temperature of 25 °C, pH 6, substrate concentration of 1.5 mM, salinity concentration of 0.1 % NaCl and incubation time 72 hrs were favourable for the production of silver nanoparticles by the three *Fusarium* isolates.

appears as a shoulder in the UV–Vis spectra. This shoulder at 378 nm corresponds to the transverse plasmon vibration in the silver nanoparticles. According to Figure 5, the variation in absorbance values after 2 hrs is not very significant, showing that the attainment of reaction equilibrium after 72 hrs and indicative of the fact that reaction came to equilibrium at about 120 hrs. An absorption band at 270 nm was observed which indicated the presence of tryptophan and tyrosine residues in proteins (Figure 6). This observation can be attributed to the capping proteins secreted by the fungus in the solution are very much stable. Other important absorption band to silver nanoparticles is at 378 nm this band appears as shoulder and corresponds to the transverse plasmon vibration in the silver nanoparticles while the peak at 420 nm is due to excitation of longitudinal plasmon vibrations. This band as well as the band around ca. 420 nm indicates the formation of silver nanoparticles. The separation between the bands indicates that silver nanoparticles are formed mostly as aggregates (Basavaraja et al., 2008).

Characterization of silver nanoparticles

Nanoparticles synthesized by different biological means are characterized using different spectroscopic techniques such as UV-Vis spectroscopy, FTIR spectroscopy, Fluorescent spectroscopy etc. Microscopic techniques such as Transmission electron microscopy, Scanning electron microscopy, Atomic force microscopy and other standard materials characterization techniques such as Energy dispersive X-ray analysis (EDX), X-ray diffraction (XRD), and Thermogravimetric analysis (TGA) have been used.

Absorbance spectra of nanoparticles to find absorbance peak (UV-Visible studies)

UV-Visible absorption spectroscopy is one of the most widely used techniques for structural characterization of silver nanoparticles. The formation and stability of silver nanoparticles in the colloidal solution was monitored by using UV–Vis spectral analysis, for which after

completion of reaction after 72 hrs haliquots of the reaction sample were removed and subjected to UV–Vis spectroscopy measurements. Fungal cell filtrate treated with silver nitrate (1.5mM) showed the sharp peak at around ca.420 nm with high absorbance (*F.oxysporum* at 4.43 nm, *F. graminearum* at 3.67 nm, *F. solani* at 3.38 nm) which is very specific for silver nanoparticles which increased in absorbance with increasing time of incubation. The obtained results are correlating with the reports of (Sadowski et al., 2008a; Sadowski et al., 2008b) and (Honary et al., 2013) with the fungus *Penicillium*. Surface plasmon peak was located at ca. 420 nm and *klebsiella pneumonia* (Minaeian et al., 2008; Mokhtari et al., 2009). The typical peak at ca.420 nm corresponds to the characteristic surface plasmon resonance of silver nanoparticles. It is well known that colloidal silver nanoparticles exhibit absorption at the wavelength from 390 to 420 nm due to Mie scattering (Kleemann, 1993). Hence, the band at ca. 420 nm can be attributed to the property of Mie scattering. This may not include the protecting agent, because the Mie scattering responds only to the silver metal (Aoki et al., 2003). The plasmon bands are broad with an absorption tail in the longer wavelengths, which could be in principle due to the size distribution of the particles (Chalmers and Griffiths, 2002). Since the varying intensity of the plasmon resonance depends on the cluster size, the number of particles cannot be related linearly to the absorbance intensities (Klabunde, 2001).

Transmission electron microscopic (TEM) image analysis

- *Fusarium oxysporum* (TA), the Transmission Electron Microscopy (TEM) visualization allows measuring the size and shape of the silver nanoparticles formed. From the TEM microscopy is shown in (Figure 7), the particles obtained exhibited a regular spherical shape with smooth surfaces and the size was distributed in a range of about 5-40 nm The frequency distribution observed from the histogram shows that almost of the particles are in the 10- to 20 nm range.
- *Fusarium graminearum* (KHG), from Figure 7 it is observed that there is variation in the particle sizes with almost 40% of the particles in 60 nm range, 30 % in 70 nm range and 20 % in 50 nm ranges. The TEM image suggests that the particles are polydisperse and are mostly spherical in shape.
- *Fusarium solani* (T18), from the TEM microscopy is shown in Figure 7 the particles obtained exhibited a regular spherical shape with smooth surfaces and the size was distributed in a range of about 5-40 nm. The frequency distribution observed from the histogram shows that almost of the particles are in the 10 to 20 nm range.

Typical bright-field TEM images of the synthesized silver nanoparticles are shown in Figure 7; they show individual silver nanoparticles as well as a number of aggregates. The morphology of the nanoparticles is highly variable. A representative TEM image recorded from drop coated film of silver nanoparticles are spherical in shape and showed a large distribution of sizes in the range of 5-80 nm. All the particles are well separated and no agglomeration was noticed, indicating stabilization of the nanoparticles by a capping agent. The process of growing silver nanoparticles comprises of two key steps: (a) bioreduction of $AgNO_3$ to produced silver nanoparticles and (b) stabilization and/or encapsulation of the same by suitable capping agents (Mukherjee et al., 2008). It is suggest that the biological molecules could possibly perform the function for the stabilization of the AgNPs. The separation between the silver nanoparticles seen in the TEM image could be due to capping by proteins and would explain the UV-Vis spectroscopy measurements, which is characteristic of well-dispersed silver nanoparticles.

X-Ray Diffraction Analysis (XRD)

It is important to know the exact nature of the silver particles formed and this can be achieved by measuring the XRD-spectrum of the samples. The XRD pattern of the as-prepared silver nanoparticles shows that they held a cubic crystal structure (Figure 8). The major strong characteristic peaks of silver nanoparticles for the three isolated at 2θ are 40.2° for *F. oxysporium*, 38.5° for *F. graminearum* and 38.5, 77.7° for *F. solani* which were corresponding to crystal faces of 111, 111 and 311 of silver nanoparticles, respectively. According to the full width at half-maximum of the diffraction peaks, the average size of the particles could be estimated from WIN-FIT program (Krumm, 1995) it appear from 5-50 nm. The intense peaks observed in the spectrum agree to the Braggs's reflection of silver nanocrystals reported in literature (64) this further confirms that the silver nanoparticles formed in the extracellular filtrate are present in the form silver nanocrystals.

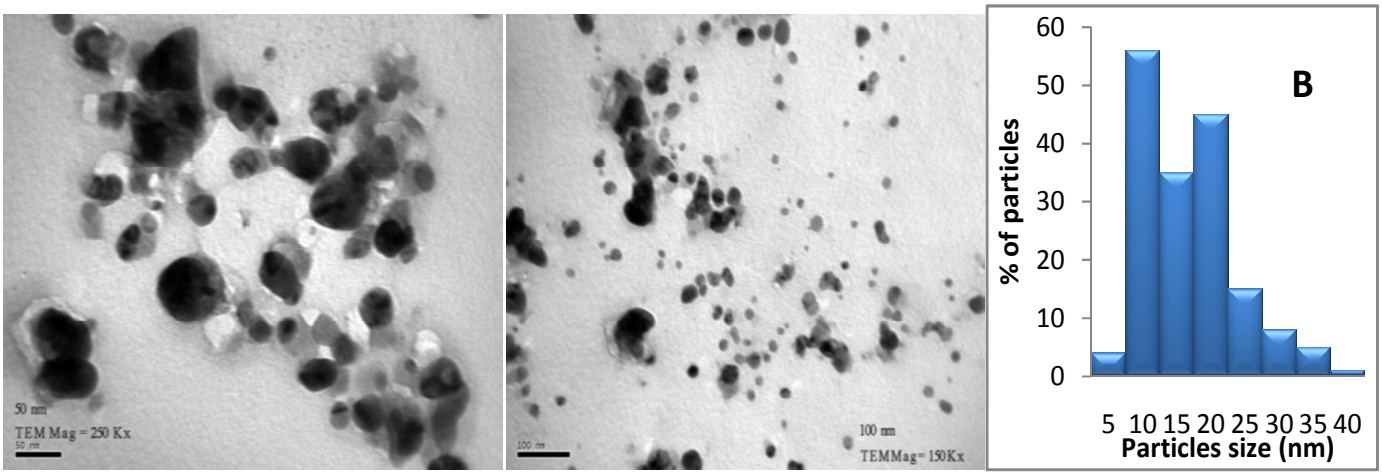

Fusarium oxysporum (TA)

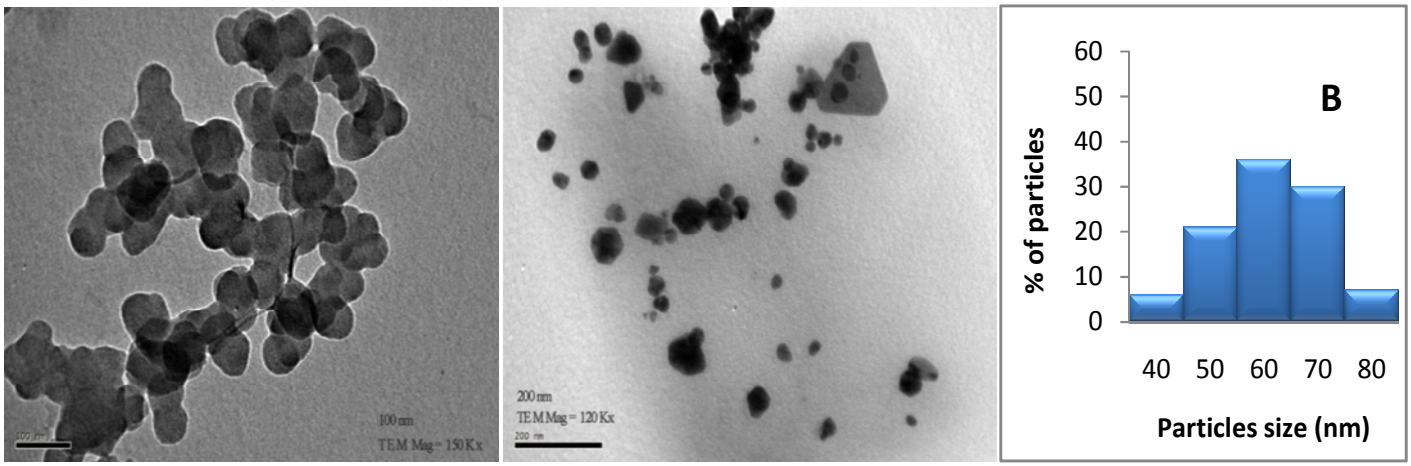

F. graminearum (KHG)

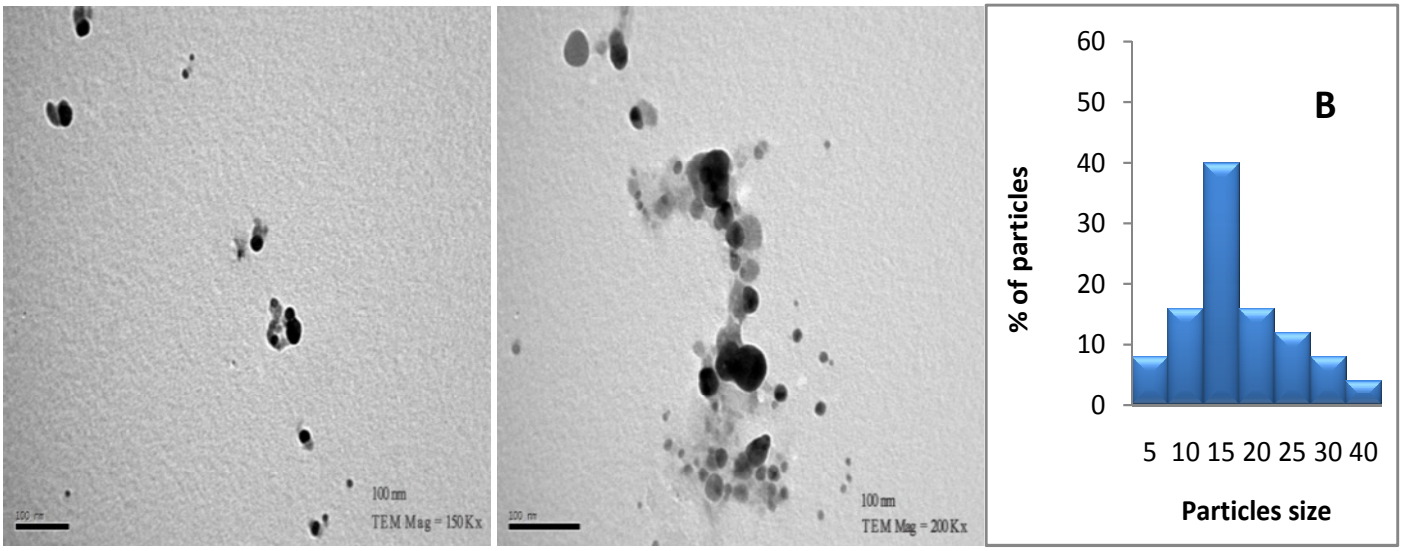

F. solani (T18)

Figure 7. Analysis of TEM micrograph of *F. oxysporum*, *F. graminearum* and *F. solani* (A) Enlarged view of TEM micrograph showing measurements, (B) Particle size distribution histogram of silver nanoparticles from transmission electron microscope (TEM) analysis.

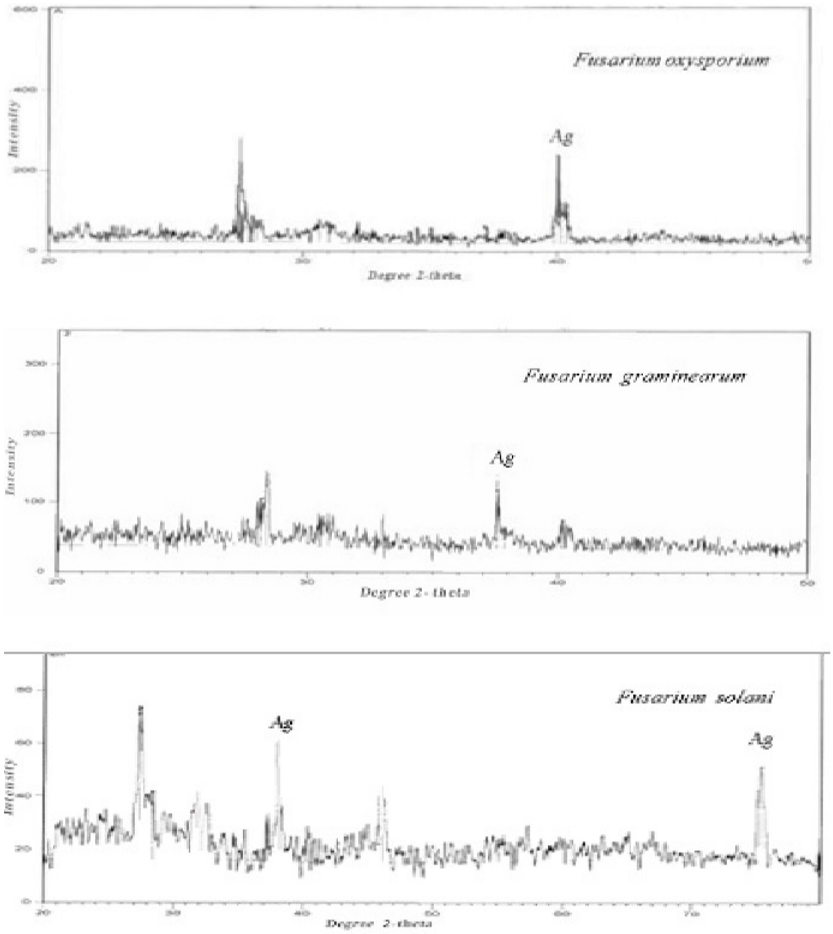

Figure 8. X-ray diffraction pattern of the dried silver nanoparticles. *F. oxysporum*, the diffraction at 40.185°, 2θ with the line width of the (111) plane of silver nanoparticles, *F. graminearum,* the diffraction at 38.5°, 2θ with the line width of the (111) plane of silver and *F. solani* , the diffractions at 38.5°, 77.74°, 2θ with the line width of the (111) , (311) planes of silver nanoparticles

Differentiation among Fusarium strains based on their protein banding patterns obtained by PAGE

The cell free filtrate was salted out overnight at 4°C using ammonium sulfate precipitation method followed by centrifugation. The precipitate fraction was subsequently dialyzed using a 12-kDa cut-off membrane. To determine the protein(s) secreted by the three *Fusarium* spp. that are responsible for trapping of the aqueous Ag^+, the extracellular proteins secreted by the three fungal in the filtrate both in the absence and presence of silver nitrate were analyzed by PAGE (Polyacrylamide Gel Electrophoresis). Fungi are very well known to secrete large amount of proteins which play a major role in their life cycle. The majority of these proteins include hydrolytic enzymes such as amylases, cellulases and proteases (Peberdy, 1994). Most of the proteomic studies have focused on the proteins involved in the metabolic pathways, however, other proteins and their role still remains unknown. The protein fraction clearly showed absence of bands (Figure 9, lane 2, 4 and 6). These proteins can be responsible for the synthesis as well as stability of silver nanoparticles (Bansal et al., 2004). Studies with *F. oxysporum* showed presence of two extracellular proteins having molecular weight of 24 and 28 kDa responsible for the synthesis of zirconia nanoparticles (Bansal et al., 2004). These protein bands, when eluted and checked on PAGE along with the proteins eluted from native PAGE, indicated that the corresponding two bands appear at the same level, thus suggesting that both proteins consist of monomeric units (Bansal et al., 2004). In order to identify the proteins bound to the surface of silver nanoparticles, the as-synthesized silver nanoparticles were treated with 0.1% SDS solution in boiling water bath. SDS act as a denaturing agent and its treatment results in detachment of the surface bounded proteins from nanoparticles. The treated and un-treated samples were analyzed by 10 %

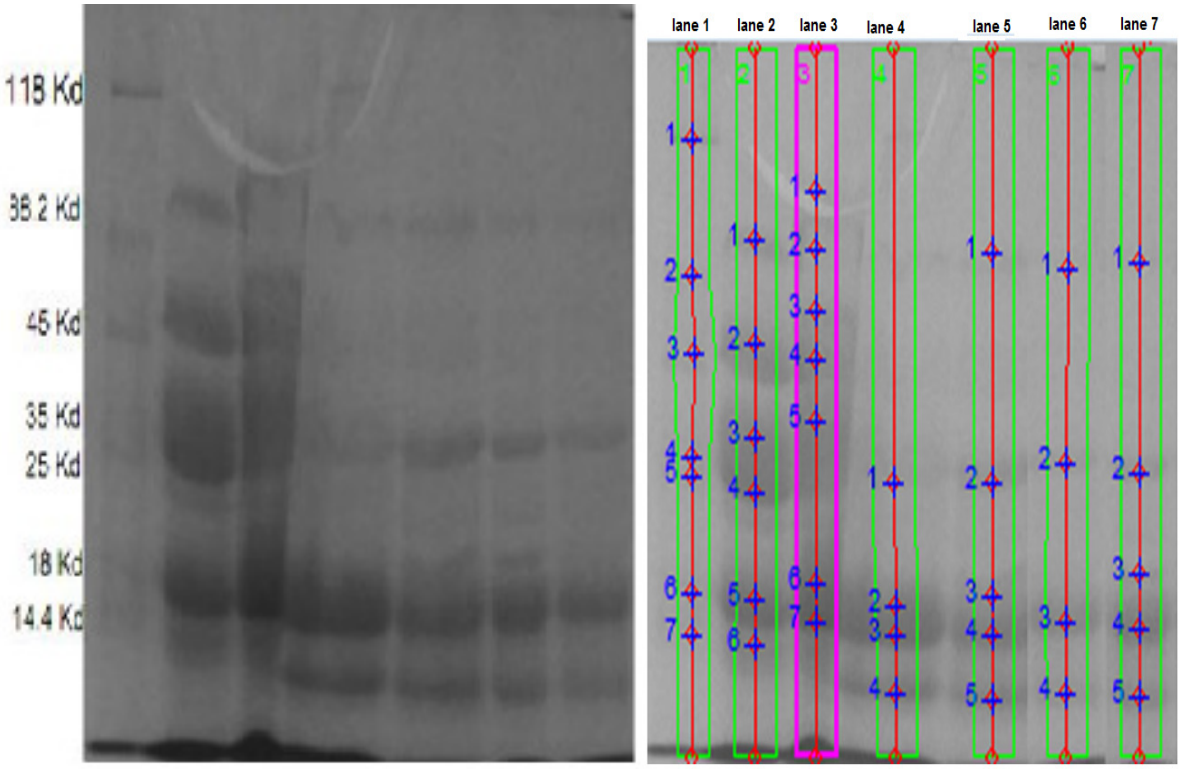

Figure 9.The profile of extracellular proteins secreted by the three *Fusarium* spp. Lane 1: shows the standard protein molecular weight markers with the corresponding molecular weights; cell-free extract of the biomass in the presence (lanes 2, 4 and 6) and absence (lanes 3, 5 and 7) of aqueous silver nitrate. Lanes 2 and 3 *F. oxysporium*; lane 4 and 5 *F. grmenarium* 6 and 7 *F. solani*, the numbers high lighting the bands indicate the proteins secreted by *Fusarium* spp.

SDS-PAGE as described earlier. An intense band was observed at the transition of the stacking and resolving gel containing untreated samples showing silver deposition. The synthesis process occurs in two steps: firstly, reduction of bulk silver ions into silver nanoparticles and, secondly, capping of the as-synthesized nanoparticles. The first step involves a 35 kDa protein which may be a reductase secreted by the fungal isolate, which may be specific for reduction of silver ions into silver nanoparticles. The second step involves 25 kDa proteins which bind with nanoparticles and confer stability. The protein-nanoparticles interactions can play a very significant role in providing stability to nanoparticles. The results obtained in our studies were similar with (Jain et al., 2011). Previous studies had also shown that the proteins bound to nanoparticle surface immediately upon contact with the nanoparticles (Elechiguerra et al., 2005). The protein adsorption has been widely studied and it has been found that protein adsorption depends on various factors such as electrostatic, hydrophobic and specific chemical interactions between the protein and the adsorbent (Lynch and Dawson, 2008).

FTIR spectrum of silver nanoparticles

Fusarium oxysporum (TA), FTIR measurements were carried out to identify the possible bimolecular responsible for the reduction of the Ag^{+} ions and capping of the bioreduced silver nanoparticles synthesized by fungal filtrate. It showed the presence of bands at 1636, 1542 and 1514 cm-1 are identified as the amide I and amide II arises due to carbonyl stretch and –N-H stretch vibrations in the amide linkages of the proteins, respectively (Figure 10).

Fusarium graminearum (KHG), The FTIR spectra reveal the presence of different functional groups like C–N, C–O–C, amide linkages and –COO–, these may be between amino acid residues in protein and synthesized silver nanoparticles. Representative spectra of obtained nanoparticles (Figure 10) manifests absorption peaks located at about 1041, 1246, 1351, 1393, 1452, 1518, 1595 and 1641, 2925, 3282 in the region 400-4000 cm^{-1}.

Fusarium solani (T18), The FTIR spectrum recorded from the freeze-dried powder of silver nanoparticles, formed after 72 hrs of incubation with the fungus. The amide linkages between amino acid residues in proteins

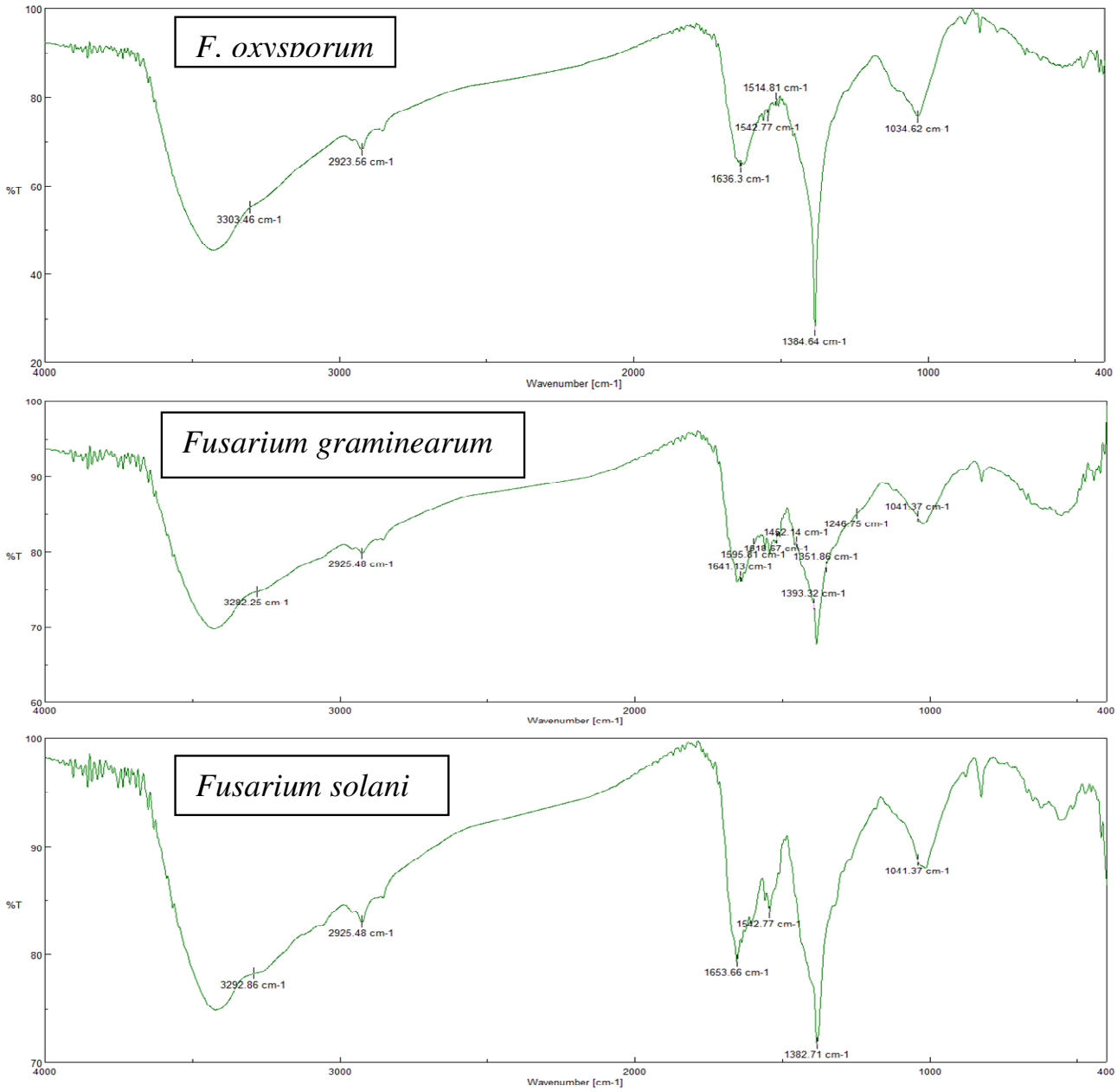

Figure 10. FTIR spectrum recorded from a drop-coated film of an aqueous solution incubated with *F. Oxysporum, Fusarium graminearum* , *Fusarium solani* and reacted with silver metal ions for 72 hrs. (T% = Transmission).

give rise to the well-known signatures in the infrared region of the electromagnetic spectrum. The bands seen at 3280 cm^{-1} and 2924 cm^{-1} were assigned to the stretching vibrations of primary and secondary amines, respectively; while their corresponding bending vibrations were seen at 1653 cm-1 and 1542 cm^{-1}, respectively. The two bands observed at 1382 cm-1 and 1041 cm-1 can be assigned to the C–Nstretching vibrations of aromatic and aliphatic amines, respectively (Figure 10). The overall observation confirms the presence of protein in the samples of silver nanoparticles.

FTIR is a powerful tool for identifying types of chemical bonds in a molecule by producing an infrared absorption spectrum that is like a molecular "fingerprint" (Senapati, 2005). The wavelength of light absorbed is characteristic of the chemical bond as can be seen in this annotated spectrum. Because the strength of the absorption is proportional to the concentration, FTIR can be used for quantitative analyses. The FTIR measurement can also be utilized to study the presence of a protein molecule in the solution, as the FTIR spectra in the 1400-1700 cm^{-1} region provides information about the presence of “C=O”

and “N-H” groups (Senapati et al., 2005). The main goal of FTIR in this study is to determine the chemical functional groups in the sample (Senapati, 2005; Senapati et al., 2005). The results obtained from FTIR in our studies were similar with (Mukerjee et al., 2001a; Oksanen et al., 2000). Representative spectra of obtained nanoparticles manifests absorption peaks located at about 1,040, 1,240, 1,280, 1,350, 1,390, 1,452, 1,515, 1,595 and 1,630, in the region 1,000–1,800 cm-1. The FTIR spectra reveal the presence of different functional groups like C–N, C–O–C, amide linkages and –COO–, these may be between amino acid residues in protein and synthesized silver nanoparticles, which give rise to the well-known signatures in the infrared region of the electromagnetic spectrum. The positions of these bands are close to that reported in literature for native proteins (Oksanen et al., 2000).The bands seen at 3280 cm−1 and 2924 cm−1 were assigned to the stretching vibrations of primary and secondary amines, (Carrasco et al., 2005; Vigneshwaran et al., 2006). Our findings corroborate (Gole et al., 200l), who reported that proteins can bind to nanoparticles either through free amine groups or cysteine residues in the proteins and through the electrostatic attraction of negatively charged carboxylate groups in enzymes present in the cell wall of mycelia and therefore, stabilization of the silver nanoparticles by proteins. Similarly, (Sastry et al., 2003) and (Sanghi and Verma, 2009) have reported that bonds or functional groups such as –C– O–C–, –C–O– and –C=C– are derived from heterocyclic compounds like proteins, which are present in the fungal extract and are the capping ligands of the nanoparticles (Sastry et al., 2003; Sanghi and Verma, 2009). Application of the biological systems for the synthesis of silver nanoparticles has already been reported (Cao, 2004; Gade et al., 2008; Ingle et al., 2008). However, the exact reaction mechanism leading to the formation of silver nanoparticles by all these organisms is yet to be elucidated. (Ahmad et al., 2002) have reported that certain NADH dependent reductase was involved in the reduction of silver ions in case of *F. oxysporum*, which later confirmed by (Anilkumar et al., 2007). This study gives the evidence of formation and stabilization of silver nanoparticles in the aqueous medium by using biological molecules. Thus, the FTIR measurement indicates that the secondary structure of proteins is not affected because of its interaction with Ag^+ ions or nanoparticles.

CONCLUSION

In the present study, we focused on biosynthesis of silver nanoparticles using *Fusarium* spp. On combining all optimized conditions, ecofriendly and inexpensive method has been developed for the rapid and large scale synthesis of SNPs, All three isolates *F. oxysporum*, *F. graminearum* and *F. solani* showed ability to biosynthesis of nanosilver. Parametric optimization studies revealed that temperature of 25 ^{o}C, pH 6, substrate concentration of 1.5 mM, salinity concentration of 0.1 % NaCl and incubation time 72 hrs was favorable for the production of silver nanoparticles by three *Fusarium* isolates.

Fungal cell filtrate treated with silver nitrate (1.5 mM) showed the sharp peak at around ca. 420 nm with high absorbance (*F. oxysporum* at 4.43 nm, *F. graminearum* at 3.67 nm and *F. solani* at 3.38 nm) The average size of the nanoparticles was estimated to be 5-80 nm, the XRD pattern of the as-prepared Ag nanoparticles shows that they held a cubic crystal structure, the protein fraction clearly showed absence of bands in the cell filtrate treated with silver nitrate (1.5 mM) compared to untreated filtrate, The possibility of protein as a stabilizing material in silver nanoparticles is revealed by FTIR analysis which show presence of two bands at 1636, 1542 and 1514 cm-1 are identified as the amide I and amide II arises due to carbonyl stretch and -N-H stretch vibrations in the amide linkages of the proteins, respectively.

ACKNOWLEDGMENTS

My deep thanks to colleagues of the Agricultural Microbiology Department National Research Centre and Prof. Dr. Gamal Saeid Mohamed Elbahy Professor of physics, National Research Centre for her help and support throughout the work.

REFERENCE

Abou El-N MM, Eftaiha A, Al-Warthan A, Ammar RAA (2010). The Arabian Journal of Chemistry 3:135–140

Ahmad A, Mukherjee P, Mandal D, Senapati S, Khan MI, Kumar R, Sastry M (2002). J Journal of the American Chemical Society, 8:124-121.

Ahmad A, Mukherjee P, Senapati S, Mandal D, Khan MI, Kumar R, Sastry M (2003). Colloids Surface B: Biointerfaces, 28:313-318.

Ahmad T, Wani IA, Manzoor N, Ahmed J, Asiri AM (2013). Collo Surf B: Biointerfaces 107:227–234

Anilkumar S, Abyaneh MK, Gosavi SW, Kulkarni SK, Pasricha R, Ahmad A, Khan MI (2007). Biotechnology Letters, 29:439-445.

Aoki K, Chen J, Yang N, Nagasawa H (2003). Langmuir, 19:9904-9909.

Auffan M, Rose J, Bottero JY, Lowry GV, Jolivet JP, MR (2009). Nature Nanotechnology, 4(10):634-641.

Balaji DS, Basavaraja S, Deshpande R, Mahesh DB, Prabhakar BK, Venkataraman A (2009). Colloids Surface B: Biointerfaces, 68:88-92.

Bansal V, Ramanathan R, Bhargava SK (2011). Australian Journal of Chemistry. 64:279–293

Bansal V, Rautaray D, Ahmad A, Sastry M (2004). Journal of Materials Chemistry, 14:3303-3305.

Basavaraja S, Balaji SD, Lagashetty A, Rajasab AH, Venkataraman A (2008). Materials Research Bulletin, 43:1164-1170.

Binupriya AR, Sathishkumar M, Yun SI (2010). Colloids and Surfaces B: Biointerfaces, 79:531-534.

Birla SS, Tiwari VV, Gade AK, Ingle AP, Yadav AP, Rai MK (2009). Letters in Applied Microbiology, 48:173–179.

Cao G (2004). Imperial College Press, London, 13: 978-981.

Carrasco F, Pages P, Lacorte T, Briceno K (2005). Journal of Applied Polymer Science, 98:1524-1535.

Chalmers JM, Griffiths PR (2002). Wiley-Interscience, 1:1369-1385.
Chepuri RK, Trivedi DC (2005). Synthetic Metals, 155:324-327.
Chladek G, Mertas A, Barszczewska-Rybarek I (2011). International Journal of Molecular Sciences, 12:4735–4744.
Courrol LC, Oliveira FR, Gomes L (2007). Engineering Aspects, 305:54-57.
Du L, Xian L, Feng J (2011). Journal of Nanoparticles Research, 13:921-930.
Durán N, Marcato PD, Alves OL, De Souza GHI, Esposito E (2005). *Journal* of Biomaterials and Nanobiotechnology, 3:1-8.
Elechiguerra JL, Burt JL, Morones JR, Camacho-Bragado A, Gao X, Lara HH, Yacaman MJ (2005). Journal of Nanobiotechnology, 3:1-10.
Elfatih M, Ali K, Inanaga S, Sugimoto Y (2002). Phytopathol. Mediterr, 41:163–169.
Gade AK, Bonde P, Ingle AP, Marcato PD, Duran N, Rai MK (2008). The Journal of *Biobased* Materials Bioenergy, 2:243-247.
Gole AC, Dash V, Ramakrishnan SR, Sainkar AB, Mandale M, Sastry M (200l). Langmuir, 17:1674-1679.
Gupta S, Devi S. K. Journal of Basic Microbiology, 51:1-6.
Haware MP, Nene YL, Pundir RPS (1992). J. Narayana, Field Crops Research, 30:147-154.
He R, Qian X, Yin J, Zhu Z (2002). Journal of Materials Chemistry 12:3783-3786.
Honary S, Barabadi H, Gharaei-Fathabad E, Naghibi F (2013). Tropical Journal of Pharmaceutical Research, 12(1):7-11.
Ingle A, Gade A, Pierrat S, Sonnichsen C, Rai M (2008). Current Nanoscience, 4:141-144.
Ingle A, Rai M, Gate A, Bawaskar M (2009). The Journal of Nanoparticles Research, 11:2079-2085.
Jain N, Bhargava A, Majumdar S, Tarafdarb JC, Panwar J (2011). The Royal Society of Chemistry, 3:635-641.
Jo HJ, Choi JW, Lee Hong SH (2012). Journal of Hazardous Materials 227:301–308
Joerger R, Klaus T (2000). CG Granqvist, Advanced Materials, 12:407-409.
Kathiresan K, Manivannan S, Nabeel MA, Dhivya B (2009). Colloids Surface B Biointerfaces, 71:133-137.
Klabunde KJ (2001). Wiley-Interscience, 7:162-170.
Kleemann W (1993). International Journal of *Modern* Physics B, 38:16-21.
Knetsch MLW, Koole LH (2011). Polymers, 3:340–366.
KokuraS, Handa O, Takagi T, Ishikawa T, Naito Y, Yoshikawa T (2010). Nanomedicine, 6:570–574.
Krumm S (1995). WINFIT1.0 - A Computer Program for X-ray Diffraction Line Profile Analysis. Acta Universitatis Carolinae, 38:253-261.
Laemmli UK (1970). Nature, 227: 680-685.
Lara HH, Garza-Trevi˜no EN, Ixtepan-Turrent L, DK (2011). Journal of Nanobiotechnology, 145:83–96.
Leslie JF, Summerell BA (2006). Blackwell. Publishing-Wiley, Hoboken, NJ.
Li T, Park HG, Choi SH (2007). Materials Chemistry and Physics, 105:325-330.
Lu HW, Liu XL, Wang SH, Qian XF, Yin J, Jhu JK (2003). Materials Chemistry and Physics, 81:104- 107.
Lynch I, Dawson KA (2008). Nano Today, 3:40-47.
Minaeian S, Shahverdi RA, Nohi SA, Shahverdi RH (2008). The Journal of the Iowa Academy of Science, 17:1-4.
Mokhtari N, Daneshpajouh S, Seyedbagheri S, Atashdehghan R, Abdi K, Sarkar S, Minaian S, Shahverdi HR, Shahverdi AR (2009). Materials Research Bulletin, 44:1415-1421.
Mukerjee P, Ahmad A, Mandal D, Senapati S, Sainkar SR, Khan MI, Parischa R, Ajayakumar PV, Alam M, Kumar R, Sastry M (2001a). Nano Letter, 1:515-519.
Mukerjee P, Ahmad A, Mandal D, Senapati S, Sainkar SR, Khan MI, Ramani R, Parischa R, Ajayakumar PV, Alam M, Sastry M, Kumar R (2001b). *Angewandte* Chemie International Edition, 40(19):3585-3588.
Mukherjee P, Roy M, Dey GK, Mukherjee PK, Ghatak J, Tyagi AK, Kale SP (2008). Nanotechnology. 19 (7):1-7
Murumkor CV, Chavan ID (1985). *Biovegyanam*, 11(1):118-120.
Narayanan KB, Park HH (2014). The European Journal of Plant Pathology, doi:10.1007/s10658-014-0399-4
Narayanan KB, Sakthivel N (2011). Advances in Colloid and Interface Science, (2011) 156:1-13.
Nel A, Xia T, Mädler L, Li N (2006). 311:622–7.
Nelson PE, Toussoun TA, Marasas WFO (1983). State University Press, University Park, 13:319-328.
Oksanen T, Pere J, Paavilainen L, Buchert J, Viikari L (2000). Journal of Biotechnology, 78(1):39-44.
Peberdy JF (1994). Trends Biotechnology, 12:50–57.
Petit C, Lixon P, Pileni MP (1993). J Ph. Chemistry, 97:12974 -12983.
Rai M, Yadav A, Bridge P, Gade A (2009). CAB International, Oxfordshire UK, 14:258–267.
Sadowski Z, Maliszewska HI, Grochowalska B, Polowczyk I, Kozlecki T (2008b). Materials Science-Poland, 26:419-424.
Sadowski Z, Maliszewska I, Polowczyk I, Kozlecki T, Grochowalska B (2008a). Polish J chemistry, 82:377-382.
Sammons DW, Adams LD, Nishizawa EE (1981). Electrophoresis, 2:135-141.
Sanghi R, Verma P (2009). Bioresource Technology, 100:501-504.
Sastry M, Ahmad A, Khan MI, Kumar R (2003). Current Science, 85:162-170.
Sastry M, Patil V, Sainkar SR (2002). Trends Biotechnology; 3(5):461 - 463.
Sathishkumar M, Sneha K, Won WS, Cho CW, Kim S, Yun YS (2009). Colloids Surfaces, Biointerfaces, 73:332- 338.
Saxena MC, Singh Saxena KB, Singh KB (eds) (1987). The Chickpea. CAB International, UK. p.127-162.
Seifert K (1996). 13:1-30.
Senapati S (2005) Ph.D. thesis, University of Pune.
Senapati S, Ahmad A, Khan MI, Sastry M, Kumar R (2005). Small, 1(5):517-520.
Sheikhloo Z, Salouti M, Katiraee F (2011). The Journal of Cluster Science, 22(4):661-665.
Sheng Z, Liu Y(2011). Water Research, 45:6039–6050.
Trop M, Novak M, Rodl S, Hellbom B, Kroell W, Goessler W (2006). The Journal of Trauma Injury, Infection and Critical Care 60:648–652. doi:10.1097/01.ta.0000208126.22089.b6
Vahabi K, Mansoori GA, Karimi S (2011). Insciences Journal1: 65–79.
Varshney R, Mishra AN, Bhadauria S, Gaur MS (2009). Digest journal of Nanomaterials and Biostructures, 4:349-355.
Verano-Braga T, Miethling-Graff R, Wojdyla K, Rogowska-Wrzesinska A, Brewer JR, Erdmann H, Kjeldsen F, Nano ACS (2014) 8(3):2161–2175
Vigneshwaran N, Ashtaputre NM, Varadarajan PV, Nachane RP, Paralikar KM, Balasubramanya RH (2006). Materials Letters, 61:1413-1418.
Wang H, Wu L, Reinhard BM, Nano ACS (2012). 6(8):7122-7132
Wiesner MR, Lowry GV, Alvarez P, Dionysiou D, Biswas P (2006). Enviromental Sceince Technology, 40(14):4336-4345.
Williams DB (1996). Material Science, Plenum Press, 4:571-625.
Xie J, Lee JY, Wang DIC, Ting YP (2007). The Journal of Physical Chemistry *C,* 111:16858-16865.
Yehia RS, Al-Sheikh H (2014). World J Microbiol Biotechnology, DOI 10.1007/s11274-014-1703-3